

IN SAR-Based Digital Elevation Model (DEM) Improvement Using Data Fusion Technique with Neural Networks on Diverse Topographic Indian Regions

Priyank Girdhik Ashutosh Bhardwaj

INDIAN INSTITUTE OF REMOTE SENSING (IIRS), DEO, CHANAKYANAGAR, INDIA

ABSTRACT

The Synthetic Aperture Radar (SAR) imaging is a remote sensing technique or the SAR imaging provides an accurate technique of monitoring various the geospatial high-contrast features. SAR is a remote sensing technique a large number of topographic information acquisition, very high contrast of the digital data being captured as the SAR output of the processing. The synthetic aperture radar (SAR) imaging is a remote sensing technique that is developed to be used in the SAR imaging. The SAR imaging is a remote sensing technique that is developed to be used in the SAR imaging. The SAR imaging is a remote sensing technique that is developed to be used in the SAR imaging.

CPRI

INTRODUCTION

The Synthetic Aperture Radar (SAR) imaging is a remote sensing technique or the SAR imaging provides an accurate technique of monitoring various the geospatial high-contrast features. SAR is a remote sensing technique a large number of topographic information acquisition, very high contrast of the digital data being captured as the SAR output of the processing. The synthetic aperture radar (SAR) imaging is a remote sensing technique that is developed to be used in the SAR imaging. The SAR imaging is a remote sensing technique that is developed to be used in the SAR imaging. The SAR imaging is a remote sensing technique that is developed to be used in the SAR imaging.

CPRI

STUDY AREAS AND DATASETS

Figure 1. Study area map depicting the location of the study area in the Indian subcontinent. The map highlights the study area in the Indian subcontinent, showing the location of the study area in the Indian subcontinent.

The Synthetic Aperture Radar (SAR) imaging is a remote sensing technique or the SAR imaging provides an accurate technique of monitoring various the geospatial high-contrast features. SAR is a remote sensing technique a large number of topographic information acquisition, very high contrast of the digital data being captured as the SAR output of the processing. The synthetic aperture radar (SAR) imaging is a remote sensing technique that is developed to be used in the SAR imaging. The SAR imaging is a remote sensing technique that is developed to be used in the SAR imaging. The SAR imaging is a remote sensing technique that is developed to be used in the SAR imaging.

CPRI

METHOD

Figure 2. Neural Network-based DEM fusion and improvement framework for the study area.

Figure 3. Neural Network-based DEM fusion and improvement framework for the study area.

CONCLUSION

The Synthetic Aperture Radar (SAR) imaging is a remote sensing technique or the SAR imaging provides an accurate technique of monitoring various the geospatial high-contrast features. SAR is a remote sensing technique a large number of topographic information acquisition, very high contrast of the digital data being captured as the SAR output of the processing. The synthetic aperture radar (SAR) imaging is a remote sensing technique that is developed to be used in the SAR imaging. The SAR imaging is a remote sensing technique that is developed to be used in the SAR imaging. The SAR imaging is a remote sensing technique that is developed to be used in the SAR imaging.

CPRI

RESULTS AND DISCUSSIONS

Figure 4. SAR-based DEM fusion and improvement framework for the study area.

Figure 5. SAR-based DEM fusion and improvement framework for the study area.

Figure 6. SAR-based DEM fusion and improvement framework for the study area.

The Synthetic Aperture Radar (SAR) imaging is a remote sensing technique or the SAR imaging provides an accurate technique of monitoring various the geospatial high-contrast features. SAR is a remote sensing technique a large number of topographic information acquisition, very high contrast of the digital data being captured as the SAR output of the processing. The synthetic aperture radar (SAR) imaging is a remote sensing technique that is developed to be used in the SAR imaging. The SAR imaging is a remote sensing technique that is developed to be used in the SAR imaging. The SAR imaging is a remote sensing technique that is developed to be used in the SAR imaging.

CPRI

CONCLUSION AND REFERENCES

The Synthetic Aperture Radar (SAR) imaging is a remote sensing technique or the SAR imaging provides an accurate technique of monitoring various the geospatial high-contrast features. SAR is a remote sensing technique a large number of topographic information acquisition, very high contrast of the digital data being captured as the SAR output of the processing. The synthetic aperture radar (SAR) imaging is a remote sensing technique that is developed to be used in the SAR imaging. The SAR imaging is a remote sensing technique that is developed to be used in the SAR imaging. The SAR imaging is a remote sensing technique that is developed to be used in the SAR imaging.

CPRI, CHANAKYANAGAR, DEO, INDIA | CPRI, CHANAKYANAGAR, DEO, INDIA | CPRI, CHANAKYANAGAR, DEO, INDIA | CPRI, CHANAKYANAGAR, DEO, INDIA | CPRI, CHANAKYANAGAR, DEO, INDIA

INDIAN INSTITUTE OF REMOTE SENSING (IIRS), ISRO, DEHRADUN, INDIA



PRESENTED AT:

AGU FALL MEETING
Chicago, IL & Online Everywhere
12–16 December 2022

SCIENCE LEADS THE FUTURE



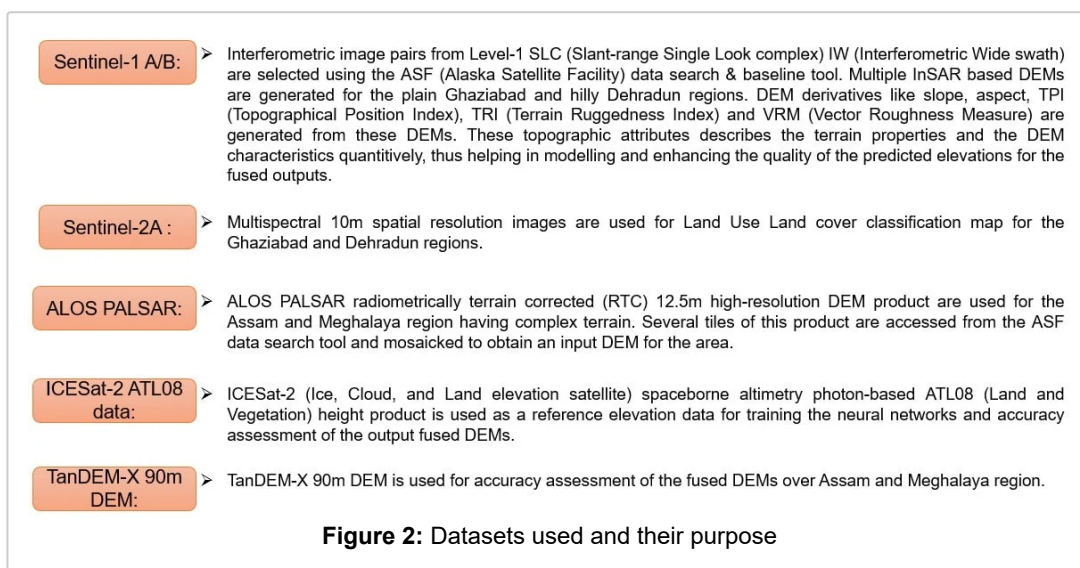
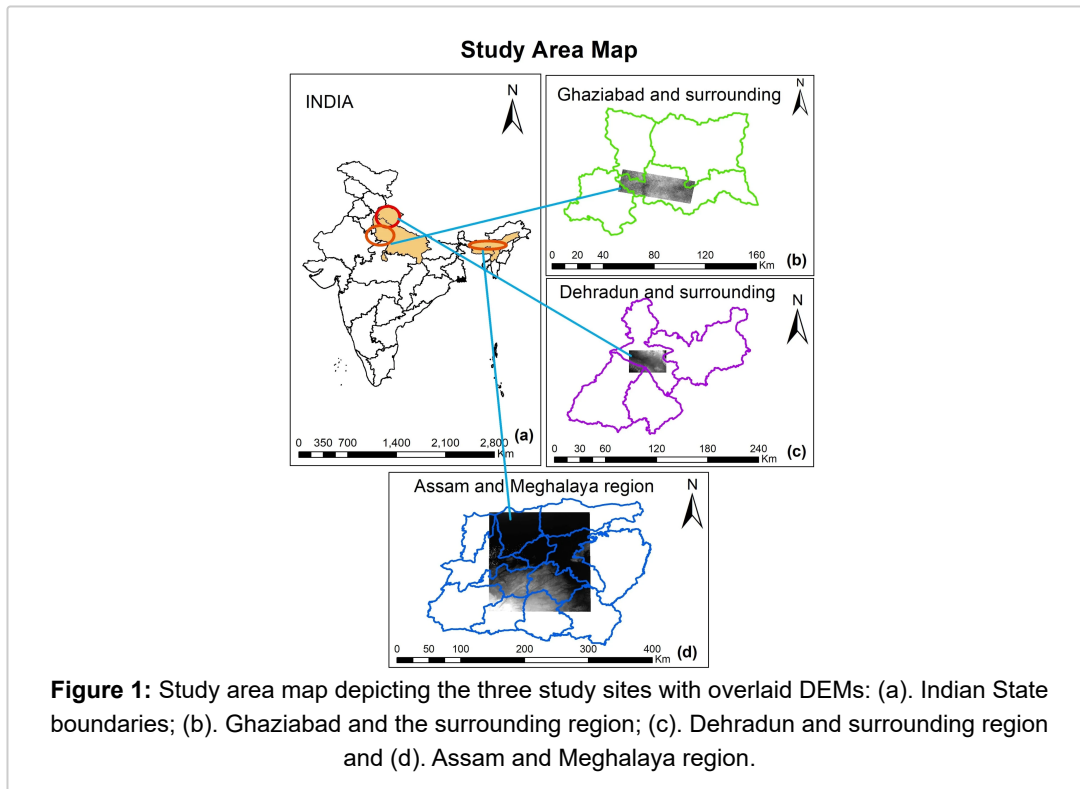
ABSTRACT

The Synthetic Aperture Radar (SAR) operating in the microwave portion of the EM spectrum provides an advanced technique of Interferometry (InSAR) for generating high-spatial-resolution DEMs. DEMs serve as an important input to a large number of topographic and modeling applications. Any improvement in the input using data fusion will add value to the output of these applications. The universal approximation and adaptive learning of the neural networks pave the way for developing a fusion framework for the improvement of these elevation models. The Feed-Forward Backpropagation neural network model is trained using training samples for different topographic terrains, one is Ghaziabad which is a plain area and the other is the Dehradun region which is a hilly terrain area. The elevation values from multiple input InSAR-based DEMs generated using Sentinel-1A/B images and values of DEM derivatives such as slope, aspect, topographic position index (TPI), terrain ruggedness index (TRI), vector roughness measure (VRM) are used along with Land Use Land Cover (LULC) classes information from Sentinel-2A multispectral data, for the preparation of training samples. The reference elevation used for training is obtained from the ICESat-2 ATL08 Land and Vegetation height product. By removing outliers and using hyperparameter optimization for selecting the best fit neural network architecture, the models are trained. The plain terrain model uses a Log-sigmoid with a simpler structure while the hilly terrain uses a linear activation function with more neurons in hidden layers. The trained models produce fused DEMs on the test areas and an accuracy analysis is performed. The root mean square error (RMSE) is estimated for evaluating the obtained fused DEMs with the TanDEM-X 90m DEM. A more complex mountainous terrain is selected from the north-eastern Himalayan portions of the Assam and Meghalaya region, where two ALOS PALSAR Radiometrically Terrain Corrected (RTC) 12m high-resolution DEMs are fused and improved using the neural network fusion framework. The fused output DEMs shows improvement with lower RMSE values as compared to the individual input DEMs. The plain terrain has 4.34m; hilly terrain shows 10.95m and mountainous terrain has 7m RMSE which is very low in comparison to the individual DEMs RMSE.

INTRODUCTION

SAR Interferometry (InSAR) is an advanced technique for obtaining high-spatial-resolution topographic models referred to as Digital Elevation Models (DEMs). DEMs are the three-dimensional representation of the earth's surface topography using either a gridded-raster form or a vectorised TIN form. The DEM is an essential and crucial input element of various applications that includes hydrology, glaciology, forestry, agriculture, urban planning and environmental monitoring studies. An automatic approach to improve the quality of the DEMs by combining them intelligently can be derived by utilizing the learning abilities of the artificial neural networks (ANNs) from the external environment. The Feed-Forward multilayer neural networks are employed with the backpropagation algorithms. With the speciality of universal approximation and abilities to handle non-linear data, a Neural Network based fusion framework is designed for efficiently performing DEM fusion and its improvement over diverse terrains of the Indian sites. Three different terrains plain, hilly and complex, are selected for this study. Different ANN structures are implemented using programming and MATLAB Neural Network (NN) toolbox. The input feature vector constitutes the elevation values from multiple InSAR DEMs generated from Sentinel-1A/B image pairs for plain and hilly study sites along with the DEM derivatives and LULC information for that area. The DEM derivatives used while training the models help in modelling the relationship between the input elevation and the reference elevations. While ALOS PALSAR RTC 12.5m DEM products are used for the third complex terrain site. The precise ICESat-2 ATL08 Land and Vegetation height product provides for the reference elevations or the known output for the training of the NN models. Applying heuristics and performing hyperparameter optimization for selecting the best architecture, the NN models are trained by applying a sufficient number of training samples for each area. The Neural Networks once trained successfully using the training and validation data, are tested on the new data samples from the test areas and the fused elevation output from the models is obtained. The NN models provide the predictions for elevation values of the fused DEMs by learning the terrain properties from the provided training samples. This work is relevant in the context of various topographical and quantitative modelling applications where the DEMs serve as a primary input. Improved input applied to an application will produce better-quality output.

STUDY AREAS AND DATASETS



Study areas:

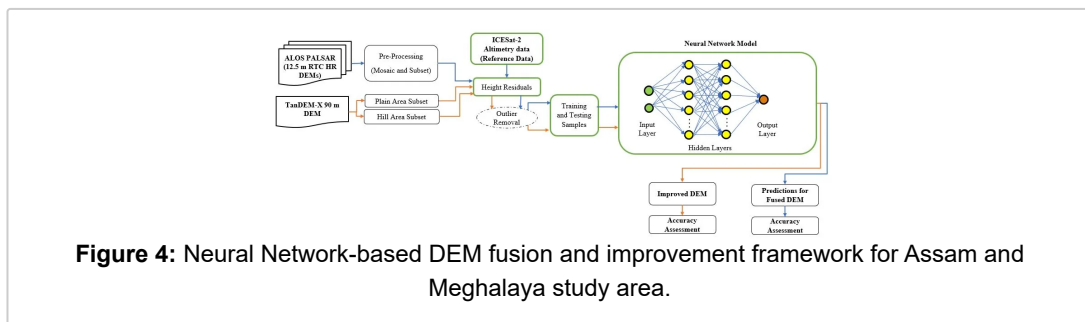
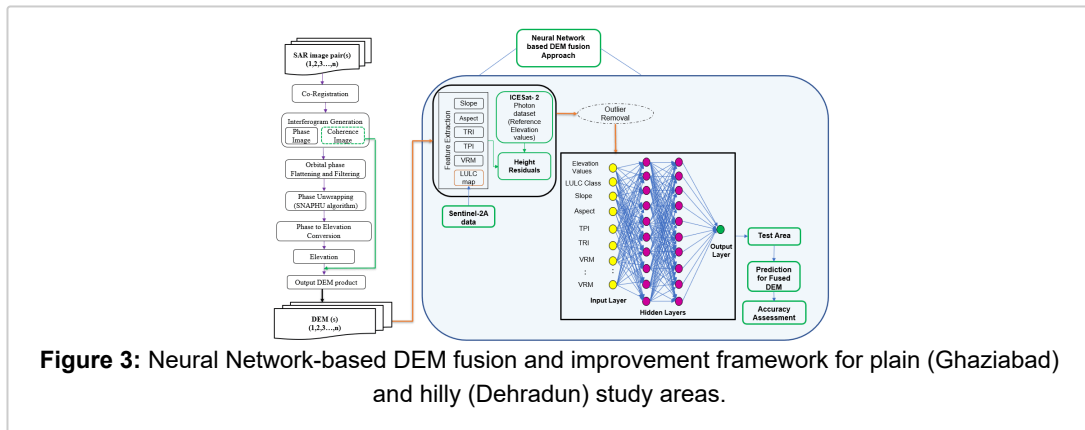
(a). Ghaziabad and its surroundings: The first study area is from Ghaziabad and its surrounding regions from the state of Uttar Pradesh. This is a relatively plain terrain region. The InSAR DEM overlaid on the study area (figure1.b) shows the geographical extent covering from 77° to 78° E Latitude and 28° to 29° N Longitude, that is an area of 777.9 sq. Km. The average elevation of this area is around 214m and the values range from 60m in the eastern part to 300m in the northwest parts. The climate is tropical monsoon type and the terrain relief is featureless with fertile land. This region includes highly dense-urban and rural built-up settlements. Other LULC classes include agricultural fields, croplands, barren lands, roads-highways, and a river body.

(b). Dehradun and its surroundings: The hilly terrain region is selected from Dehradun and its surrounding regions. It is the largest, most populated, and the capital of the state of Uttarakhand. Its location is in the foothills of the Himalayas and the Shivalik range in the Doon valley. The latitude and longitude extend from 77°34' to 78°18' E and 29°58' to 31°2'

N covering an area of 3088 sq. Km. Two major rivers the Ganges and the Yamuna flow across this region. Geographically this region consists of highlands and hills with cooler temperatures and dense forest ranges. The elevation values of this hilly terrain of this region range from 410m in the town area to around 2000m in the Mussoorie hills. The land cover includes dense built-ups in the city of Dehradun surrounded by dense forest covered with large tree canopies. This region is highly vulnerable to natural disasters like seasonal floods, landslides, and earthquakes.

(c). Assam and Meghalaya regions: This study area is from the North-Eastern Himalayan region covering several districts of Assam and Meghalaya states. The geographic extent of this region covers from 25.40' to 26.85' N Latitude and 91.61' and 93.07' E Longitude. The portion of Assam has Northern Himalayas, Brahmaputra floodplains, and plateaus in the southern parts. The temperate and tropical rainforest-type climate receives heavy rainfalls and the height of hills ranges from 300m to 2000m. The Brahmaputra, older than the Himalayas, flows through this state, eroding the place and forming steep gorges and floodplains. While the Meghalaya region has a highland Shillong plateau and several faults. The region contains the oldest rocks from Precambrian to the new alluvium formations. This region observes active tectonics due to the collision of Indian & Tibetan landmasses and is of geological importance. The overall elevation values for the whole region range from 1m to around 2000m.

METHOD

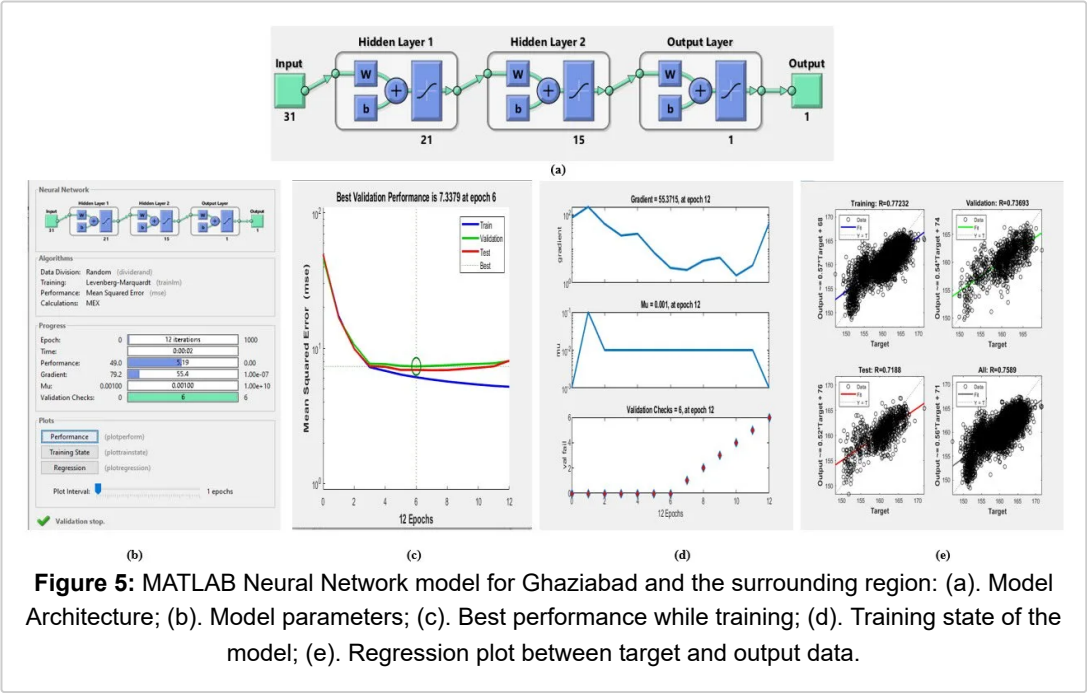


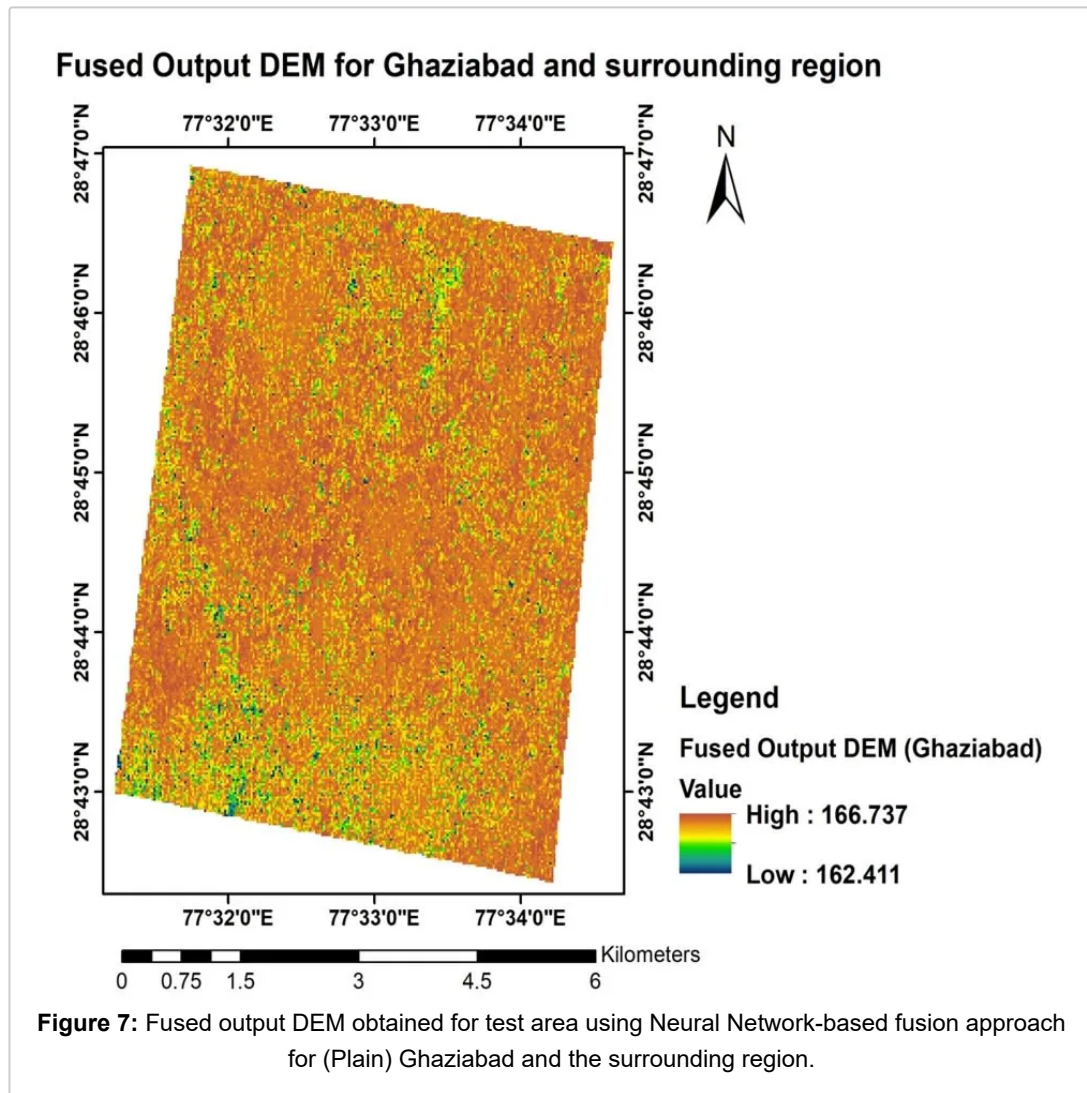
Methodology:

Multiple InSAR-based DEMs are generated using Sentinel-1A/B SAR image pairs following the interferometric process for the Ghaziabad and Dehradun study areas. These multiple DEMs are input to the different Neural Network models. DEM derivatives such as the slope, aspect, TPI (Topographical Position Index), TRI (Terrain Ruggedness Index), and VRM (Vector Roughness Measure) along with the LULC information constitute the input feature vector for the models. A simple ANN structure is designed to have an input, two hidden, and an output layer. One way to implement the neural networks is with python programming which uses Keras (Tensorflow) library. The NN models are sequential dense layer feed-forward multilayer models with gradient descent backpropagation algorithms and Adam (Adaptive Moment) optimizer. Another way is by using MATLAB Neural Network (NN) Toolbox where a faster training algorithm of Levenberg Marquardt (TRAINLM) is used for training the Feed Forward Backpropagation neural network models. The training data is filtered for outlier removal using values within the range of a second standard deviation. These are applied to the input layer of the NN models along with the reference elevations from the precise ICESat-2 ATL08 (Land and Vegetation) height product. Hyperparameter optimization is performed to select the parameters for a best-fit NN model for each study area. Thus, by selecting the suitable number of neurons, activation function, number of layers, and loss function, different NN architectures are trained using training samples and the best model is saved. The NN for both study sites has an input layer, two hidden layers, and an output layer with 31 – 21 – 15 – 1 node respectively for the plain Ghaziabad region and 31 – 64 – 128 – 1 node respectively for the hilly Dehradun region. Suitable activation functions are selected for each layer- Log-Sigmoid for plain and Linear for hilly study areas. The loss function (MSE) is observed for determining the overfitting or underfitting problems while training. The successful training of the models predicts elevation values for the test area. Similarly, for the third site of Assam and Meghalaya regions which has a complex terrain, elevation values of the ALOS PALSAR RTC 12.5m product is applied to the input layer along with the reference elevations and with Linear activation function, different NN structures are designed, for the complete region and valley and mountainous regions separately. The output elevation values of the fused DEMs from the trained models are then assessed for their accuracy by estimating the statistical parameters such as the RMSE (Root Mean Square Error), LE90 (Linear Error at 90th percentile), Mean Error (ME) and percentage improvement factor (%IF). The elevation values of the fused output DEMs are checked with the toposheets of each study area that they fall within the correct range. Due to the complex hilly terrain of this region, geometric distortions of foreshortening, layover, and shadow are present in the SAR images. The TanDEM-X 90m DEM product is improved over this region using the Neural Network models and the results are assessed by estimating the percentage improvement factor (%IF).

RESULTS AND DISCUSSIONS

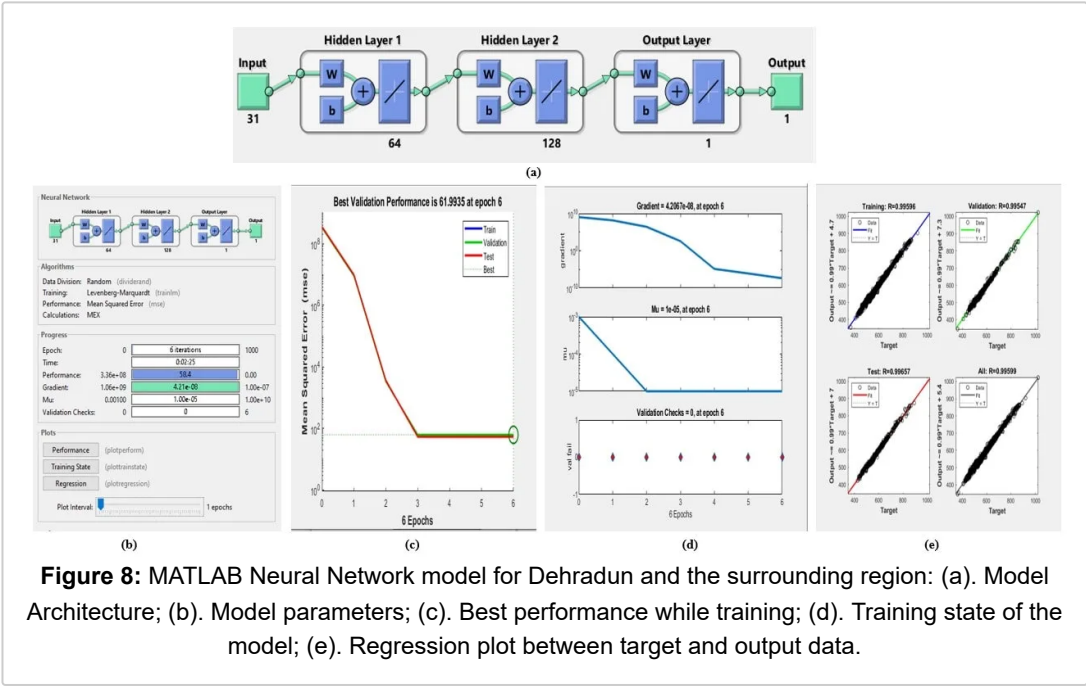
(a). Results for Ghaziabad and the surrounding region:





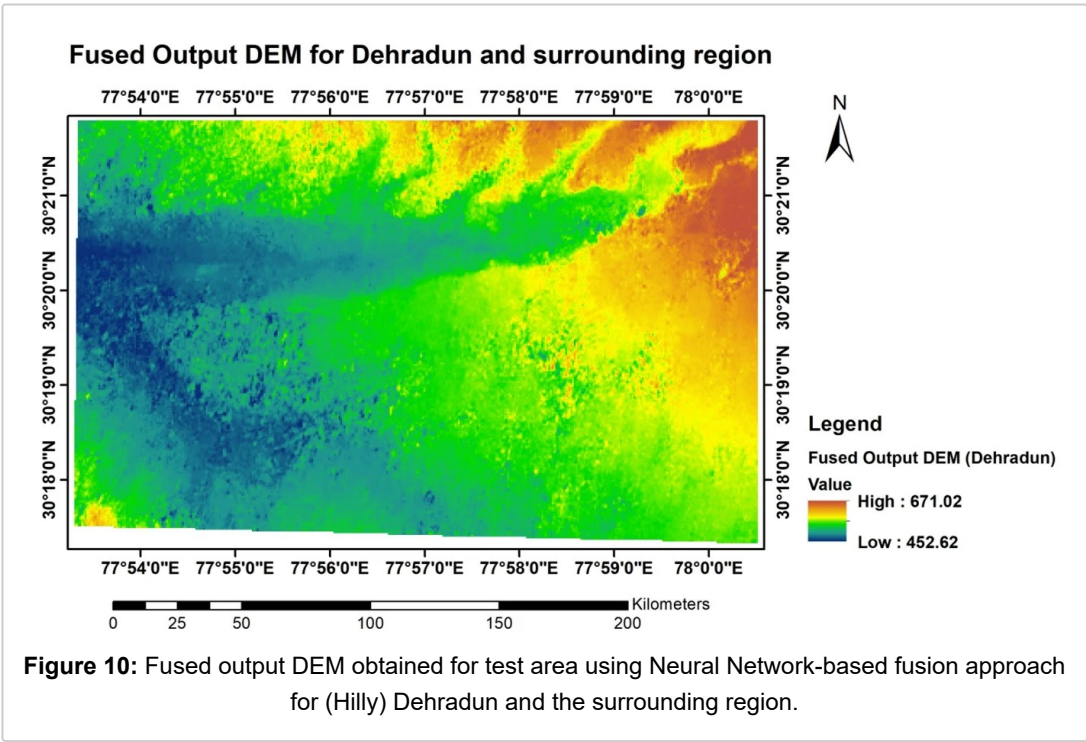
The Keras-based and the MATLAB NN-toolbox neural network model (Figure 5) uses the same structure for this plain terrain area having 31- 21- 15- 1 neuron in the input, first hidden layer, second hidden layer, and the output layer respectively. The "Sigmoid/ Log-sigmoid" activation function models this terrain appropriately. Only the training algorithm used in the MATLAB NN toolbox is TRAINLM. A total of 6694 training samples are used for training and validation of the model. After successful training, the model is simulated on the new dataset from the test area. The trained model predicts the elevation value for the fused output DEMs. The output of DEM fusion from the model is assessed with the TanDEM-X 90m DEM. The fused output DEM from the ANN model in the Ghaziabad and surrounding regions is represented by the map in Figure 7. The statistical analysis of the fused output DEM shows that the RMSE values (Figure 6) are lower around 3.46 and 4.34m for the fused DEMs in comparison to the input individual DEMs. The Linear error (LE90) is very low for the fused DEMs around 5.69 and 7.14 m for the Keras and MATLAB-based models respectively. This reveals a significant improvement of the fused DEMs in terms of accuracy over the input InSAR DEMs for the plain region obtained effectively with the use of Neural Networks.

(b). Results for Dehradun and the surrounding region:



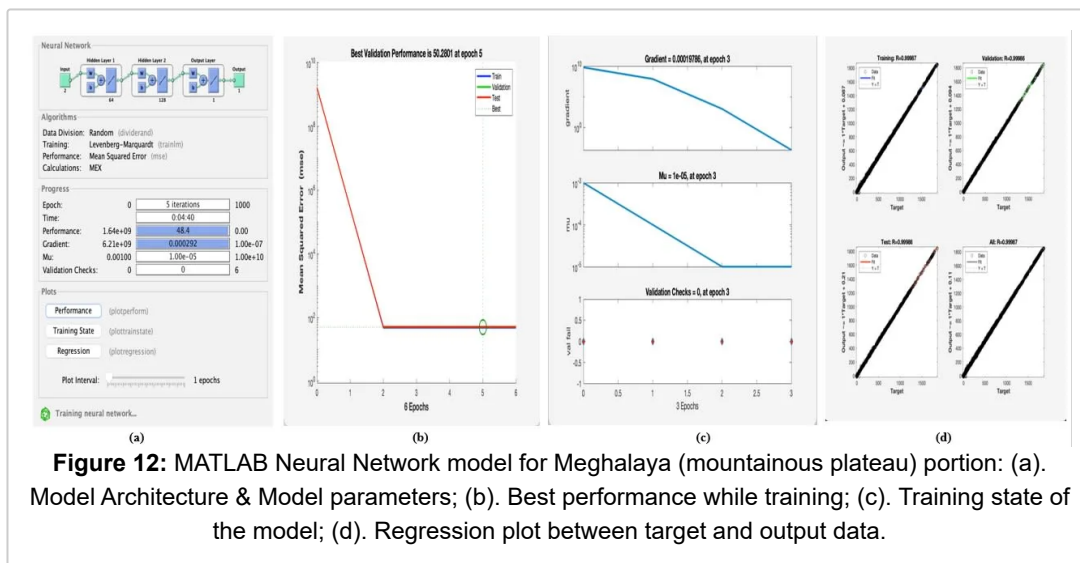
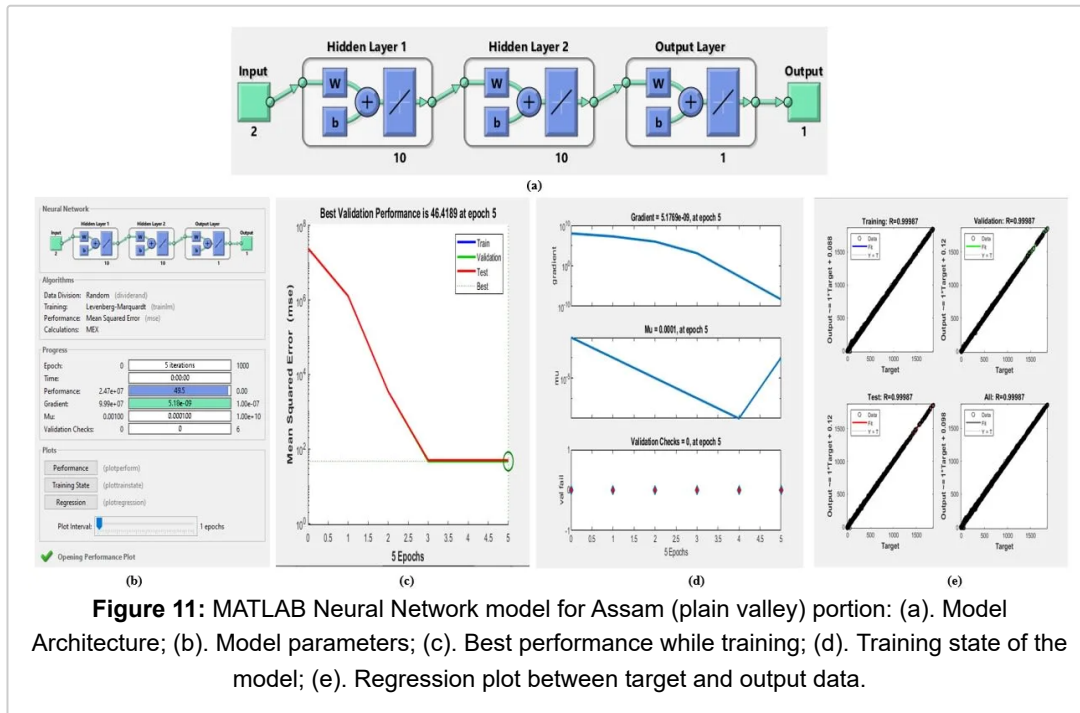
DEMs	RMSE (m)	LE90 (m)	Improvement Factor (%IF)
DEM 1	51.91	85.38	78.91
DEM 2	20.41	33.57	46.35
DEM 3	63.02	103.66	82.62
DEM 4	26.05	42.85	57.96
DEM 5	17.23	28.34	36.45
ANN Prediction (MATLAB model)	10.95	18.01	--

Figure 9: Results for Neural Network-based DEM fusion approach for Dehradun and the surrounding region.



The hilly terrain region of Dehradun and its surroundings required more neurons in each hidden layer that is 64 and 128 units for its modeling. The activation function used in this case is “Linear/PURELIN” in each model. A total of 3423 samples are used for this case after outlier removal. However, the Keras-based models were not able to produce satisfactory results on the new datasets. The MATLAB-based model (Figure 8) with a faster training algorithm, produces output fused DEM for the hilly and undulating terrain as represented in the map (Figure 10). The statistical accuracy analysis of the Fused output DEM with the TanDEM-X 90m DEM exhibits a remarkable improvement in terms of reduced RMSE and LE90 values for the fused DEMs over the input DEMs. The RMSE of fused DEMs is reduced to 10.95m as compared to the input DEMs (Figure 9).

(c). Results for Assam and Meghalaya region:



Total ICESat-2 footprints (22767 points)			
	Input DEM 1	Input DEM 2	Fused DEM
ME (m)	7.72	7.74	0.03
RMSE (m)	11.12	11.11	7.00
Plain Area (12175 Points)			
ME (m)	3.21	3.20	-0.03
RMSE (m)	5.14	5.12	3.82
Mountainous Area (10591 Points)			
ME (m)	12.91	12.95	-0.01
RMSE (m)	15.35	15.34	8.18

Figure 13: Results for Fused DEMs for Assam (plain) and Meghalaya (Mountainous) regions using ICESat-2 data.

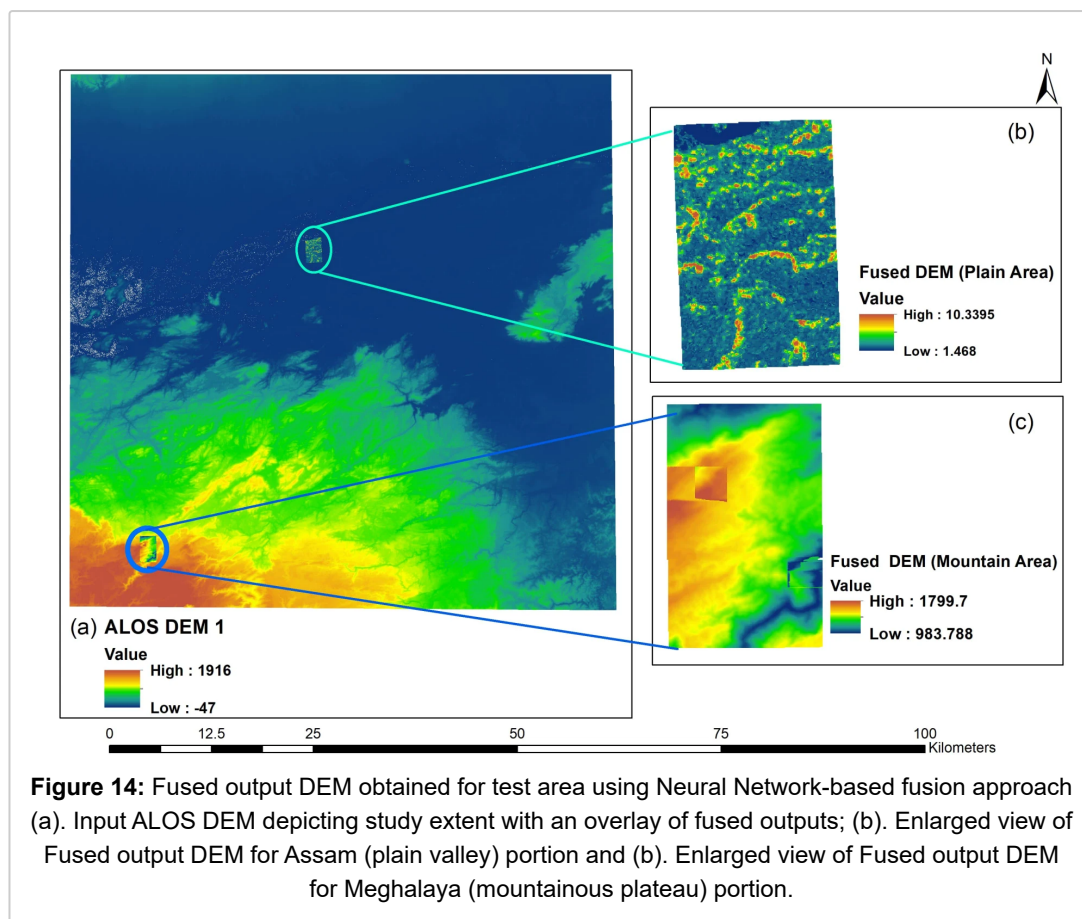


Figure 14: Fused output DEM obtained for test area using Neural Network-based fusion approach (a). Input ALOS DEM depicting study extent with an overlay of fused outputs; (b). Enlarged view of Fused output DEM for Assam (plain valley) portion and (b). Enlarged view of Fused output DEM for Meghalaya (mountainous plateau) portion.

This is a large study area with complex terrain having both a floodplain valley region in the Assam portion and a highland plateau mountainous region in the Meghalaya portion, separate models are designed for the two portions. The training and validation dataset contains total of 22767 sample points. Linear (PURELIN) activation function is used for modeling this terrain. The plain (valley) portion uses a model with structure 2-10-10-1 (Figure 11) while the mountainous portion has a model of 2-64-128-1 (Figure 12) units in the layers. The predictions for fused output DEM from the model are assessed for accuracy by calculating Mean Error (ME) and RMSE taking ICESat-2 as a reference (Figure 13). The RMSE obtained for the plain region is around 3.82m which is lower than the RMSE of 5m for the input DEMs. The fused DEM in the mountainous region has attained an RMSE of 8.18m which is remarkably low in comparison to the 15.35m value of RMSE for input DEMs.

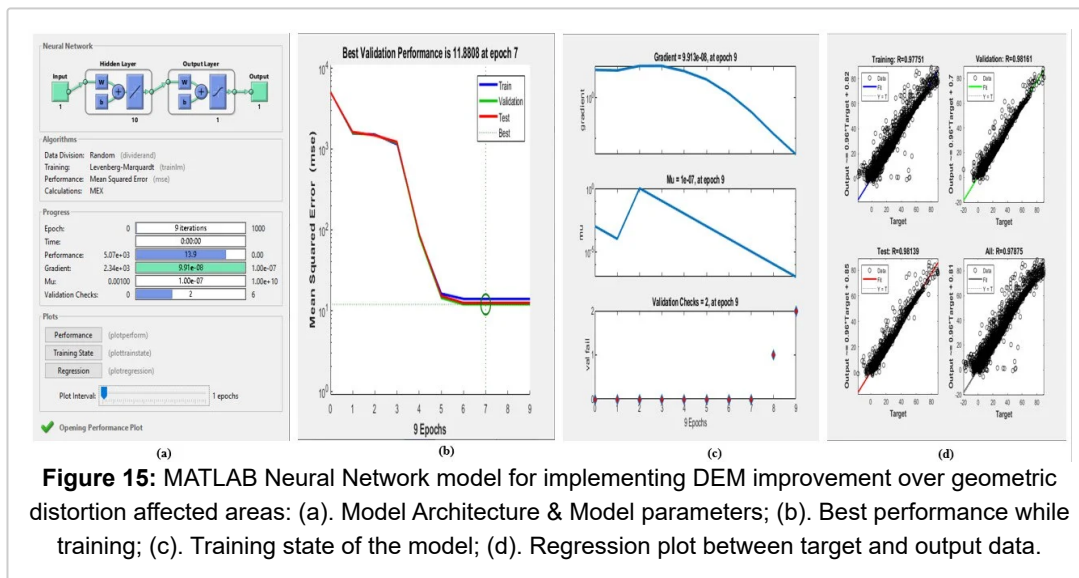
(d). Results for TanDEM-X 90m DEM improvement over geometric distortion areas:

Figure 15: MATLAB Neural Network model for implementing DEM improvement over geometric distortion affected areas: (a). Model Architecture & Model parameters; (b). Best performance while training; (c). Training state of the model; (d). Regression plot between target and output data.

Total ICESat-2 footprints (22994 points)			
	Input TDM	ANN Prediction	% IF
RMSE (m)	11.21	7.42	33.83
Plain Area Points			
RMSE (m)	4.64	3.64	21.57
Mountainous Area Points:			
RMSE (m)	14.07	8.85	37.13
Near Ground Points (having 0 to 0.5 m height error)			
Plain Area Points:			
RMSE (m)	0.26	0.14	46.76
Mountainous Area Points			
RMSE (m)	0.29	0.13	54.59

Figure 16: Results for the TanDEM-X 90m DEM in Assam and Meghalaya region

A separate model is trained with input as the elevations (22994 samples) from the TanDEM-X 90m DEM, with a simple structure of 1-10-1 neurons and linear activation function. Accuracy assessment of the results shows a significant 33.8% improvement for the geometric distortion-affected areas. Separately for the Plain portions, the improvement factor is about 21.57% while in mountainous portions the percentage improvement is around 37.13%. Further, for near-ground points (having height error between 0 to 0.5m) the TanDEM-X 90m DEM is improved upto 46.76% in the plain portion while 54.59% of improvement is achieved in the mountainous regions.

CONCLUSION AND REFERENCES

The study concludes that the Neural Network-based DEM fusion and improvement framework is an effective approach for improving the quality of the InSAR-based DEMs over diverse terrains of the Indian region. Different structures are required for modeling the relationship between input elevations and the reference elevation for different types of terrain. The plain type terrain uses lesser neurons while the hilly or mountainous terrain uses more neurons. The ANN-based DEM fusion is performed and the model learns the terrain characteristics from the applied input or training samples. After successful training, the model is simulated on the new datasets and predictions for the fused output DEMs are obtained. The developed data-driven neural network models efficiently perform DEM fusion and improvement over plain, hilly, and complex terrains. Significant improvements in terms of statistical parameters are observed in the three study areas. The improved accuracy infers that the implementation of this approach is successful over the three study areas. Although both approaches produce similar results, the MATLAB NN-Toolbox helps in designing ANN models faster with much faster-converging training algorithms, the Keras-based NN models employ more heuristics and customized approaches where suitable architecture can be iteratively tested for specific terrain. Finally, the developed models performed effectively well in obtaining improved and better quality DEMs over the plain, hilly and complex terrains of the Indian region.

REFERENCES:

1. Woodhouse, I.H. Introduction to Microwave Remote Sensing; Taylor & Francies Group: Boca Raton, FL, USA, 2006.
2. Louise, A.J.v.; Keiko, S.; Michel, M.; Don, M. Digital Elevation Models. 2007. Available online: <http://hdl.handle.net/10986/34445>. (accessed on 18 October 2021).
3. Ferretti, A.; Monti-guarnieri, A.; Prati, C.; Rocca, F.; Massonnet, D. InSAR Principles: Guidelines for SAR Interferometry Processing and Interpretation; European Space Agency: Paris, France, February, 2007.
4. Michelle Sneed, "Interferometric Synthetic Aperture Radar (InSAR)," USGS, Land Subsidence in California, 2018. Available online: https://www.usgs.gov/centers/ca-water-ls/science/interferometric-synthetic-aperture-radar-insar?qt-science_center_objects=0#qt-science_center_objects. (accessed on 7 September 2021).
5. Braun, A. (2021): Retrieval of digital elevation models from Sentinel-1 radar data – open applications, techniques, and limitations. Open Geosciences, 13(1), 532-569. doi:10.1515/geo-2020-0246.
6. Fukumori, I. Data Assimilation by Models. In International Geophysics; Academic Press: Cambridge, MA, USA, 2001; pp. 237–265.
7. Papasaika, H.; Poli, D.; Baltsavias, E. Fusion of Digital Elevation Models from Various Data Sources. In Proceedings of the 2009 International Conference on Advanced Geographic Information Systems & Web Services, Cancun, Mexico, 1–7 February 2009; pp. 117–122. <https://doi.org/10.1109/geows.2009.22>.
8. Fuss, C.E. Digital Elevation Model Generation and Fusion. Master Thesis, 2013; p. 159. Available online: https://atrium.lib.uoguelph.ca/xmlui/bitstream/handle/10214/7571/Fuss_Colleen_201309_Msc.pdf?sequence=3. (accessed on 21 October 2021).
9. A. Bhardwaj, K. Jain, and R. S. Chatterjee, "Generation of high-quality digital elevation models by assimilation of remote sensing-based DEMs," J. Appl. Remote Sens., vol. 13, no. 04, p. 1, 2019, doi: 10.1117/1.jrs.13.4.044502.
10. Papasaika, H.; Kokiopoulou, E.; Baltsavias, E.; Schindler, K.; Kressner, D. Fusion of Digital Elevation Models Using Sparse Representations. In ISPRS Conference on Photogrammetric Image Analysis; Springer: Berlin, Heidelberg, 2011; Volume 6952, pp. 171–184. https://doi.org/10.1007/978-3-642-24393-6_15.

11. Bagheri, H.; Schmitt, M.; Zhu, X.X. Fusion of TanDEM-X and Cartosat-1 elevation data supported by neural network-predicted weight maps. *ISPRS J. Photogramm. Remote Sens.* 2018, 144, 285–297. <https://doi.org/10.1016/j.isprsjprs.2018.07.007>.
12. Kim, D.E.; Liong, S.-Y.; Gourbesville, P.; Andres, L.; Liu, J. Simple-Yet-Effective SRTM DEM Improvement Scheme for Dense Urban Cities Using ANN and Remote Sensing Data: Application to Flood Modeling. *Water* 2020, 12, 816. <https://doi.org/10.3390/w12030816>.
13. Kulp, S.A.; Strauss, B.H. CoastalDEM: A global coastal digital elevation model improved from SRTM using a neural network. *Remote Sens. Environ.* 2018, 206, 231–239. <https://doi.org/10.1016/j.rse.2017.12.026>.
14. Hu, Y.H.; Hwang, J.N. *Handbook of Neural Network Signal Processing*; Academic Press, Inc.: San Diego, NY, USA, 2001.
15. Anderson, J.A. *Introduction to neural networks*, 8th ed.; MIT Press: Cambridge, MA, USA, 1994; Volume 6.
16. Kanungo, D.; Arora, M.; Sarkar, S.; Gupta, R. A comparative study of conventional, ANN black box, fuzzy and combined neural and fuzzy weighting procedures for landslide susceptibility zonation in Darjeeling Himalayas. *Eng. Geol.* 2006, 85, 347–366. <https://doi.org/10.1016/j.enggeo.2006.03.004>.
17. Kavzoglu, T.; Mather, P.M. The use of backpropagating artificial neural networks in land cover classification. *Int. J. Remote Sens.* 2003, 24, 4907–4938. <https://doi.org/10.1080/0143116031000114851>.
18. Demuth, H.; Beale, M. “Neural Network Toolbox Version4,” *Networks*, 2002; Volume 24, No. 1, pp. 1–8. Available online: <http://citeseerx.ist.psu.edu/viewdoc/download?doi=10.1.1.123.6691&rep=rep1&type=pdf> (accessed on 2 January 2022).
19. Tian, X.; Shan, J. Comprehensive Evaluation of the ICESat-2 ATL08 Terrain Product. *IEEE Trans. Geosci. Remote Sens.* 2021, 59, 8195–8209. <https://doi.org/10.1109/tgrs.2021.3051086>.
20. K. P. A. Neuenschwander, “ICESat-2 ATL08 ATBD,” 2021. https://icesat-2.gsfc.nasa.gov/sites/default/files/page_files/ICESat2_ATL08_ATBD_r004.pdf (accessed Dec. 29, 2021).
21. T. Markus et al., “The Ice, Cloud, and land Elevation Satellite-2 (ICESat-2): Science requirements, concept, and implementation,” *Remote Sens. Environ.*, vol. 190, pp. 260–273, 2017, doi: 10.1016/j.rse.2016.12.029.
22. Brown, M.E.; Arias, S.D.; Neumann, T.; Jasinski, M.F.; Posey, P.; Babonis, G.; Glenn, N.F.; Birkett, C.M.; Escobar, V.M.; Markus, T. Applications for ICESat-2 Data: From NASA's Early Adopter Program. *IEEE Geosci. Remote Sens. Mag.* 2016, 4, 24–37. <https://doi.org/10.1109/mgrs.2016.2560759>.
23. Wessel, B.; Huber, M.; Wohlfart, C.; Marschall, U.; Kosmann, D.; Roth, A. Accuracy assessment of the global TanDEM-X Digital Elevation Model with GPS data. *ISPRS J. Photogramm. Remote Sens.* 2018, 139, 171–182. <https://doi.org/10.1016/j.isprsjprs.2018.02.017>.
24. A. Bhardwaj, “Quality Assessment of merged NASADEM products for varied Topographies in India using Ground Control Points from GNSS,” *MOL2NET 2020, Int. Conf. Multidiscip. Sci.* 6th Ed., no. January, pp. 2–11, 2021, [Online]. Available: <https://mol2net-06.sciforum.net/#section1478>.
25. A. Bhardwaj, “Quality Assessment of Openly Accessible Fused EarthEnvDEM90 DEM and its comparison with MERIT DEM using Ground Control Points for Diverse Topographic Regions,” *MOL2NET, Int. Conf. Ser. Multidiscip. Sci.* 6th Ed., pp. 1–8, 2020, [Online]. Available: <https://sciforum.net/paper/view/conference/6855>.
26. J. Höhle and M. Höhle, “Accuracy assessment of digital elevation models by means of robust statistical methods,” *ISPRS J. Photogramm. Remote Sens.*, vol. 64, no. 4, pp. 398–406, 2009, doi: 10.1016/j.isprsjprs.2009.02.003.
27. J. L. Mesa-Mingorance and F. J. Ariza-López, “Accuracy assessment of digital elevation models (DEMs): A critical review of practices of the past three decades,” *Remote Sens.*, vol. 12, no. 16, pp. 1–27, 2020, doi: 10.3390/RS12162630.
28. H. Karabörk, H. B. Makineci, O. Orhan, and P. Karakus, “Accuracy Assessment of DEMs Derived from Multiple SAR Data Using the InSAR Technique,” *Arab. J. Sci. Eng.*, vol. 46, no. 6, pp. 5755–5765, 2021, doi: 10.1007/s13369-020-05128-8.

DISCLOSURES

The authors have no conflicts of interest to declare that are relevant to the content of this article.

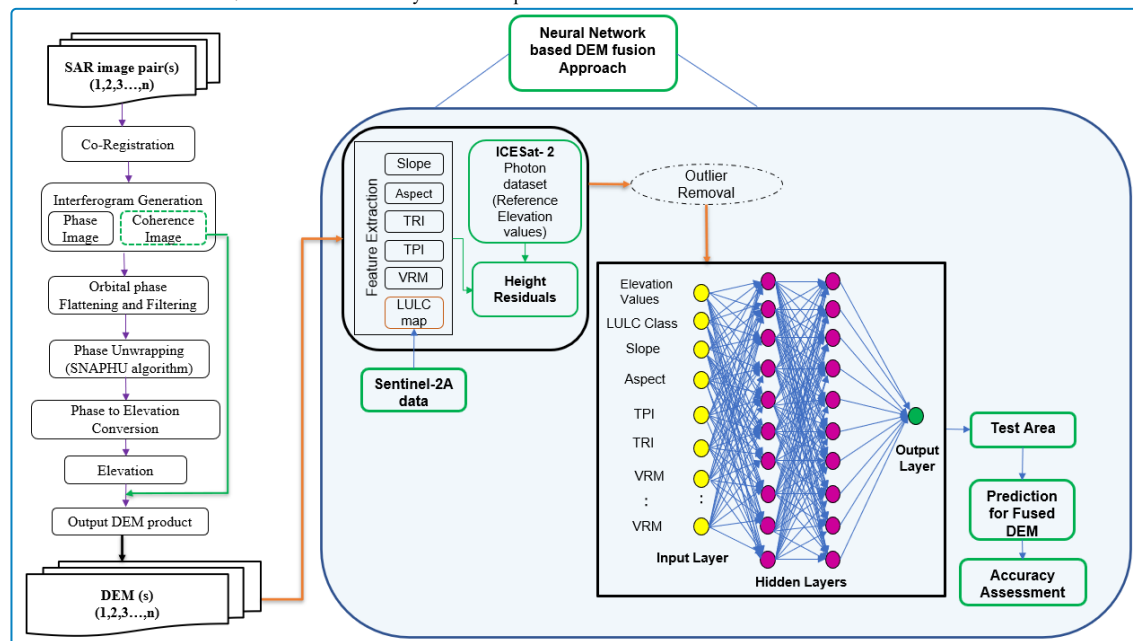
AUTHOR INFORMATION

Priti Girohi: Ms. Priti Girohi is a young research scholar in the remote sensing and GIS domain. She was born in Ghaziabad, Uttar Pradesh in March, 1995. She graduated with B.Tech in Electronics and Communication Engineering with deep knowledge in radar systems, electronic circuits, microwave and antenna subjects. She is studying at the Indian Institute of Remote Sensing (IIRS), ISRO pursuing her Masters of Technology in Remote Sensing and GIS with a specialization in Satellite Image Analysis and Photogrammetry. Her areas of research interest include Satellite Image processing, Photogrammetry, SAR Interferometry, DEM Fusion techniques, application of machine learning and deep learning in the remote sensing domain. She worked on developing methods and models for InSAR-based DEM fusion and improvement in the diverse topography of the Indian region.

Ashutosh Bhardwaj: Ashutosh Bhardwaj is a senior scientist in the Photogrammetry and Remote Sensing Department, GT&OP Group, of Indian Institute of Remote Sensing (Indian Space Research Organization), Dehradun, India. He has been engaged in teaching and research in topographic modeling, photogrammetry, SAR Interferometry, LiDAR and remote sensing. He has guided more than 50 graduate and postgraduate students and is currently guiding PhD students under various research programs. He has published more than 30 research papers in journal and conferences.

ABSTRACT

The Synthetic Aperture Radar (SAR) operating in the microwave portion of the EM spectrum provides an advanced technique of Interferometry (InSAR) for generating high-spatial-resolution DEMs. DEMs serve as an important input to a large number of topographic and modelling applications. Any improvement in the input using data fusion will add value to the output of these applications. The universal approximation and adaptive learning of the neural networks pave the way for developing a fusion framework for the improvement of these elevation models. The Feed-Forward Backpropagation neural network model is trained using training samples for different topographic terrains, one is Ghaziabad which is a plain area and the other is the Dehradun region which is a hilly terrain area. The elevation values from multiple input InSAR-based DEMs generated using Sentinel-1A/B images and values of DEM derivatives such as slope, aspect, topographic position index (TPI), terrain ruggedness index (TRI), vector roughness measure (VRM) are used along with Land Use Land Cover (LULC) classes information from Sentinel-2A multispectral data, for the preparation of training samples. The reference elevation used for training is obtained from the ICESat-2 ATL08 Land and Vegetation height product. By removing outliers and using hyperparameter optimisation for selecting the best fit neural network architecture, the models are trained. The plain terrain model uses a Log-sigmoid with a simpler structure while hilly terrain uses a linear activation function with more neurons in hidden layers. The trained models produce fused DEMs on the test areas and an accuracy analysis is performed. The root mean square error (RMSE) is estimated for evaluating the obtained fused DEMs with the TanDEM-X 90m DEM. A more complex mountainous terrain is selected from the north-eastern Himalayan portions of the Assam and Meghalaya region, where two ALOS PALSAR Radiometrically Terrain Corrected (RTC) 12m high-resolution DEMs are fused and improved using the neural network fusion framework. The fused output DEMs shows improvement with lower RMSE values as compared to the individual input DEMs. The plain terrain has 4.34m; hilly terrain shows 10.95m and mountainous terrain has 7m RMSE which is very low in comparison to the individual DEMs RMSE.



(https://agu.confex.com/data/abstract/agu/fm22/9/7/Paper_1077879_abstract_973015_0.png)

REFERENCES

REFERENCES:

1. Woodhouse, I.H. Introduction to Microwave Remote Sensing; Taylor & Francies Group: Boca Raton, FL, USA, 2006.
2. Louise, A.J.v.; Keiko, S.; Michel, M.; Don, M. Digital Elevation Models. 2007. Available online: <http://hdl.handle.net/10986/34445>. (accessed on 18 October 2021).
3. Ferretti, A.; Monti-guarnieri, A.; Prati, C.; Rocca, F.; Massonnet, D. InSAR Principles: Guidelines for SAR Interferometry Processing and Interpretation; European Space Agency: Paris, France, February, 2007.
4. Michelle Sneed, "Interferometric Synthetic Aperture Radar (InSAR)," USGS, Land Subsidence in California, 2018. Available online: https://www.usgs.gov/centers/ca-water-ls/science/interferometric-synthetic-aperture-radar-insar?qt-science_center_objects=0#qt-science_center_objects. (accessed on 7 September 2021).
5. Braun, A. (2021): Retrieval of digital elevation models from Sentinel-1 radar data – open applications, techniques, and limitations. Open Geosciences, 13(1), 532-569. doi:10.1515/geo-2020-0246.
6. Fukumori, I. Data Assimilation by Models. In International Geophysics; Academic Press: Cambridge, MA, USA, 2001; pp. 237–265.
7. Papasaika, H.; Poli, D.; Baltsavias, E. Fusion of Digital Elevation Models from Various Data Sources. In Proceedings of the 2009 International Conference on Advanced Geographic Information Systems & Web Services, Cancun, Mexico, 1–7 February 2009; pp. 117–122. <https://doi.org/10.1109/geows.2009.22>.
8. Fuss, C.E. Digital Elevation Model Generation and Fusion. Master Thesis, 2013; p. 159. Available online: https://atrium.lib.uoguelph.ca/xmlui/bitstream/handle/10214/7571/Fuss_Colleen_201309_Msc.pdf?sequence=3. (accessed on 21 October 2021).
9. A. Bhardwaj, K. Jain, and R. S. Chatterjee, "Generation of high-quality digital elevation models by assimilation of remote sensing-based DEMs," J. Appl. Remote Sens., vol. 13, no. 04, p. 1, 2019, doi: 10.1117/1.jrs.13.4.044502.
10. Papasaika, H.; Kokiopoulou, E.; Baltsavias, E.; Schindler, K.; Kressner, D. Fusion of Digital Elevation Models Using Sparse Representations. In ISPRS Conference on Photogrammetric Image Analysis; Springer: Berlin, Heidelberg, 2011; Volume 6952, pp. 171–184. https://doi.org/10.1007/978-3-642-24393-6_15.
11. Bagheri, H.; Schmitt, M.; Zhu, X.X. Fusion of TanDEM-X and Cartosat-1 elevation data supported by neural network-predicted weight maps. ISPRS J. Photogramm. Remote Sens. 2018, 144, 285–297. <https://doi.org/10.1016/j.isprsjprs.2018.07.007>.
12. Kim, D.E.; Liong, S.-Y.; Gourbesville, P.; Andres, L.; Liu, J. Simple-Yet-Effective SRTM DEM Improvement Scheme for Dense Urban Cities Using ANN and Remote Sensing Data: Application to Flood Modeling. Water 2020, 12, 816. <https://doi.org/10.3390/w12030816>.
13. Kulp, S.A.; Strauss, B.H. CoastalDEM: A global coastal digital elevation model improved from SRTM using a neural network. Remote Sens. Environ. 2018, 206, 231–239. <https://doi.org/10.1016/j.rse.2017.12.026>.
14. Hu, Y.H.; Hwang, J.N. Handbook of Neural Network Signal Processing; Academic Press, Inc.: San Diego, NY, USA, 2001.
15. Anderson, J.A. Introduction to neural networks, 8th ed.; MIT Press: Cambridge, MA, USA, 1994; Volume 6.
16. Kanungo, D.; Arora, M.; Sarkar, S.; Gupta, R. A comparative study of conventional, ANN black box, fuzzy and combined neural and fuzzy weighting procedures for landslide susceptibility zonation in Darjeeling Himalayas. Eng. Geol. 2006, 85, 347–366. <https://doi.org/10.1016/j.enggeo.2006.03.004>.
17. Kavzoglu, T.; Mather, P.M. The use of backpropagating artificial neural networks in land cover classification. Int. J. Remote Sens. 2003, 24, 4907–4938. <https://doi.org/10.1080/0143116031000114851>.
18. Demuth, H.; Beale, M. "Neural Network Toolbox Version 4," Networks, 2002; Volume 24, No. 1, pp. 1–8. Available online: <http://citeseerx.ist.psu.edu/viewdoc/download?doi=10.1.1.123.6691&rep=rep1&type=pdf> (accessed on 2 January 2022).
19. Tian, X.; Shan, J. Comprehensive Evaluation of the ICESat-2 ATL08 Terrain Product. IEEE Trans. Geosci. Remote Sens. 2021, 59, 8195–8209. <https://doi.org/10.1109/tgrs.2021.3051086>.
20. K. P. A. Neuenschwander, "ICESat-2 ATL08 ATBD," 2021. https://icesat-2.gsfc.nasa.gov/sites/default/files/page_files/ICESat2_ATL08_ATBD_r004.pdf (accessed Dec. 29, 2021).
21. T. Markus et al., "The Ice, Cloud, and land Elevation Satellite-2 (ICESat-2): Science requirements, concept, and implementation," Remote Sens. Environ., vol. 190, pp. 260–273, 2017, doi: 10.1016/j.rse.2016.12.029.
22. Brown, M.E.; Arias, S.D.; Neumann, T.; Jasinski, M.F.; Posey, P.; Babonis, G.; Glenn, N.F.; Birkett, C.M.; Escobar, V.M.; Markus, T. Applications for ICESat-2 Data: From NASA's Early Adopter Program. IEEE Geosci. Remote Sens. Mag. 2016, 4, 24–37. <https://doi.org/10.1109/mgrs.2016.2560759>.
23. Wessel, B.; Huber, M.; Wohlfart, C.; Marschall, U.; Kosmann, D.; Roth, A. Accuracy assessment of the global TanDEM-X Digital Elevation Model with GPS data. ISPRS J. Photogramm. Remote Sens. 2018, 139, 171–182. <https://doi.org/10.1016/j.isprsjprs.2018.02.017>.

24. A. Bhardwaj, "Quality Assessment of merged NASADEM products for varied Topographies in India using Ground Control Points from GNSS," MOL2NET 2020, Int. Conf. Multidiscip. Sci. 6th Ed., no. January, pp. 2–11, 2021, [Online]. Available: <https://mol2net-06.sciforum.net/#section1478>.
25. A. Bhardwaj, "Quality Assessment of Openly Accessible Fused EarthEnvDEM90 DEM and its comparison with MERIT DEM using Ground Control Points for Diverse Topographic Regions," MOL2NET, Int. Conf. Ser. Multidiscip. Sci. 6th Ed., pp. 1–8, 2020, [Online]. Available: <https://sciforum.net/paper/view/conference/6855>.
26. J. Höhle and M. Höhle, "Accuracy assessment of digital elevation models by means of robust statistical methods," ISPRS J. Photogramm. Remote Sens., vol. 64, no. 4, pp. 398–406, 2009, doi: 10.1016/j.isprsjprs.2009.02.003.
27. J. L. Mesa-Mingorance and F. J. Ariza-López, "Accuracy assessment of digital elevation models (DEMs): A critical review of practices of the past three decades," Remote Sens., vol. 12, no. 16, pp. 1–27, 2020, doi: 10.3390/RS12162630.
28. H. Karabörk, H. B. Makineci, O. Orhan, and P. Karakus, "Accuracy Assessment of DEMs Derived from Multiple SAR Data Using the InSAR Technique," Arab. J. Sci. Eng., vol. 46, no. 6, pp. 5755–5765, 2021, doi: 10.1007/s13369-020-05128-8.

